

Thermal and Hydrological Regional Characterisation of Los Humeros and Acoculco Using Modelling Methods -H2020 GEMex Project

Damien Bonté^{1*}, Jon Limberger^{1,2}, Gianluca Gola³, Eugenio Trumphy³, Guido Giordano⁴, Thomas Kretzschmar⁵, Jan Diederik van Wees^{1,2}

1- Utrecht University, Utrecht, The Netherlands; 2- TNO, Utrecht, The Netherlands; 3- CNR, Pisa, Italy; 4- Uni. Roma 3, Roma, Italy; 5- CICESE, Ensenada, Mexico

* now at IFP Energies nouvelles, 1 et 4 avenue de Bois-Préau, 92852 Rueil-Malmaison, France (damien.bonte@ifpen.fr)

Keywords: Numerical Modelling, Thermal structure, Hydrogeology, Mexico

ABSTRACT

The GEMex project is a collaborative effort between Mexican and European research institutes to develop the understanding of Enhanced Geothermal Systems (EGS) and SuperHot Geothermal Systems (SHGS). For this purpose, two volcanic sites have been selected: Los Humeros and Acoculco. Both sites are volcanically active or have experienced volcanic activity recently, including caldera formation at some point in their history. In Acoculco, the recently published work of Avellán et al. (2018) show the latest knowledge on the evolution of the volcanic system. In Los Humeros, Carrasco-Núñez et al. (2017) present a reinterpreted history of the whole system. However, while Los Humeros has experienced strong hydrothermal activity, Acoculco is presently considered as a dry system. In the frame of this GEMex project thermal models have been developed for both sites and a hydrothermal model in Los Humeros. The thermal models rely on 3D geological models, also developed in GEMex and information such as rock properties (also being acquired within GEMex) and temperature data (limited in Acoculco and more extensive but regrouped in Los Humeros). In Los Humeros, a fast and efficient thermal modelling methodology was applied, considering the regional heat source and advection related to regional groundwater flow and local high permeability zones. The hydrogeology in Los Humeros has been specifically modelled based on groundwater flow in the limestone basement, taking into consideration the heat source below the volcanic system. In Acoculco, given the scarce temperature information available, work has focused on investigating the geometry of the heat source and the resulting thermal structure. Results from geological and thermal model coupled with petrophysical rock properties are used for the resources assessment of the two sites. A common computation, based on volume method, was applied on both areas in order to obtain the thermal energy stored in the underground (Heat in Place). A better understanding of the nature of the Los Humeros and Acoculco geothermal systems is key for sustainable and safe production and for future geothermal exploration and development.

1. INTRODUCTION

Los Humeros and Acoculco are both large volcanic complex with a long-lasting history including one or several. Both situated at the Far East end of the Trans-Mexican Volcanic Belt, about 200 km north-west of Mexico City. Both sites have developed on a crystalline basement overlain by Cretaceous and Jurassic Limestone. In this work, we are defining new understanding of the thermal system from its source to the transport processes.

1.1 Los Humeros geological framework

Los Humeros volcanic complex (LHVC) is an active volcanic system (Fig. 1) with an active geothermal system located at the eastern end of the Trans-Mexican Volcanic Belt (TMVB), a volcanic arc that runs east-west as a result of the subduction of the Rivera and Cocos oceanic plates under the North American plate. The LHVC is the most northern volcano of the Serdán-Oriental Basin (SOB). LHVC is a Pleistocene basalt-andesite-rhyolite caldera that has developed on top of a crystalline basement of and a marine Cretaceous limestone (Carrasco-Núñez et al., 2017).

According to the most recent analysis of Carrasco-Núñez et al. (2018), the current volcanological formation, the caldera, has been formed in three stages. The first stage (pre-caldera) was of rhyolitic composition and place between 683.0 ± 1.7 ky and to 270 ± 15 ky. Following this ~400 kyr activity, the second stage created the main caldera of Los Humeros of 21 by 15 km at 164 ky and is associated with the emplacement of a large ignimbrite due to a large explosive eruption. At the third stage (post-caldera stage), started 50 ky ago and 4 ky. Within these 50 kyr of post-caldera evolution, the compositions have changed from rhyodacitic and dacitic tuffs to basaltic andesitic and basaltic olivine-bearing lavas, reflecting an heterogeneous magmatic source.

The resulting sequence of deposition in the LHVC as been described by Calcagno et al. (2018), with three main groups that have been identified: Pre-Caldera, Caldera, Post-Caldera. Based on their composition these groups have been further subdivided in eight units. In addition to these volcanic units and groups a basement layer has been describe that encapsulate the Palaeozoic granites and schists as well as the Jurassic and Cretaceous limestone.

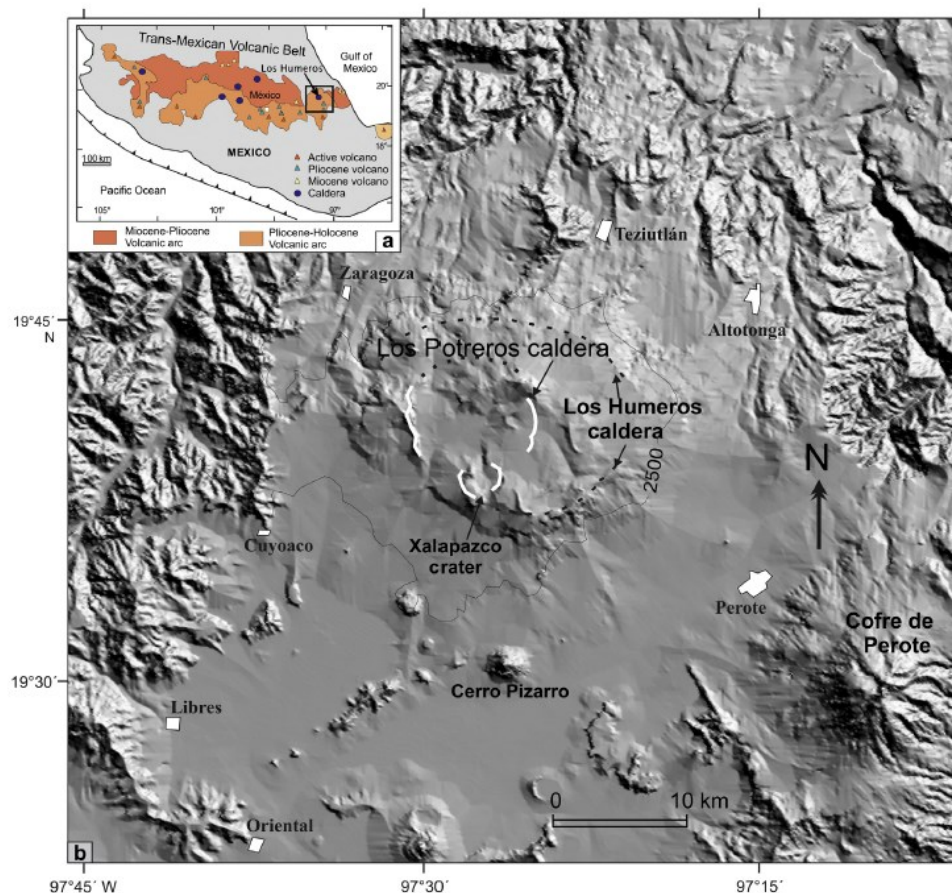


Figure 1: Location of Los Humeros caldera and geothermal field. a) Inset map showing the distribution in the eastern Trans Mexican Volcanic Belt (TMVB). b) Digital Elevation Model for Los Humeros showing the main structural features (Los Potreros and Los Humeros scarps) – from Carrasco-Núñez et al. (2017).

The faults in the Los Humeros area can be separated into regional faults that runs beyond the LHVC and the faults that results from the volcanic activity. Regional faults that affect the basement with an orientation NE-SW and NW-SE have been created through two main events; the first one (late Cretaceous to Palaeocene) was compressional and the second one (Eocene-Pleistocene) was extensional. The caldera -related faults (see Fig. 2) are the border faults both of Los Humeros and Los Potreros calderas and the NNW-SSE central faults

1.2 Acoculco geological framework

The Acoculco Caldera Complex is located in the eastern part of the Trans-Mexican Volcanic Belt. The Acoculco Caldera was formed 2.7 Ma, and since then, volcanic activity has persisted until 0.06 Ma, through the emission of domes, cinder cones, fissure lava flows and two ignimbrite eruptions dated at 1.2 and 0.65 Ma. After the caldera collapse 2.7 Ma, the local stress field was probably modified and allowed the ascent of peralkaline magmas through new plumbing systems. Such magmas mixed with calc-alkaline magmas and formed the post-caldera volcanism (Sosa-Ceballos et al., 2018). The Acoculco caldera rests upon sedimentary marine Cretaceous limestones of the Sierra Madre Oriental, and Miocene volcanic rocks belonging to early stages of the Trans-Mexican Volcanic Belt. The Cretaceous limestones do not crop out inside the Acoculco caldera but were cut in the geothermal exploration drill-holes of CFE, from 800 to 1200 m of depth in well EAC1, and from 350 to 450 m of depth in well EAC-2. Limestones with chert bands are exposed to the east of the town of Chignahuapan. The Acoculco caldera succession is also interbedded with deposits of the Apan-Tezontepac Volcanic Field that consists of 280 scoria cones, 10 shield volcanoes, and 5 domes. Most volcanoes are made of basaltic andesitic lavas with phenocrysts of olivine and plagioclase, and dacitic domes. The age of the ATVF spans from at least 2.25 ± 0.04 Ma to the Holocene (Avellán et al., 2018) (for an overview of the geological map of Acoculco see the map in Avellán et al., 2018). The Acoculco caldera rocks in the area are deformed by three main fault systems: the NE-striking Tenochtitlán-Apan fault system, and the NW-striking Tulancingo-Tlaxco fault system. Locally, the Tenochtitlán-Apan fault system is represented by the Apan-Tlaloc and Chignahuapan faults, and the Tulancingo-Tlaxco fault system is represented by the Manzanito fault. The NE- and NW-striking normal fault systems intersect each other, creating an orthogonal arrangement of grabens, half-grabens and horsts (Sosa-Ceballos et al 2018). The pervasive hydrothermal alteration in the central part of the Acoculco caldera has motivated considerable geothermal exploration. In the above mentioned exploration wells (i.e., EAC1 and EAC2) the temperature of $300\text{ }^{\circ}\text{C}$ at 2 km depth was measured, but no exploitable fluid has been discovered. Preliminary geological studies consider the site a candidate for the application of EGS technology to develop the field (Lorenzo-Pulido et al., 2010; Canet et al., 2015a). According to these studies, the geothermal target is probably located in the basement composed of calcareous, granitic and metamorphic rocks, since the overlying volcanic rocks show intense hydrothermal alteration (Calcagno et al., 2018).

2. REGIONAL TEMPERATURE STRUCTURE OF LOS HUMEROS

2.1 Data input for the model

2.1.1 Temperature

The temperature in Los Humeros is constrained by the location of the wells at the centre of the caldera. In total 65 deep wells have been drilled in Los Humeros to explore or exploit the geothermal system. The temperature information retrievable from these wells is of three types: (1) temperature log series made of measurements every 6 hours for the first 24 hours after the drilling of the wells, (2) temperature log measured after weeks or months after drilling, and (3) temperature log while the well flows.

The data from the time series in the wells has been kindly provided by the Comisión Federal de Electricidad (CFE). Within the 65 wells that have been drilled in Los Humeros, 52 were provided for investigation by the CFE leading to exploitable information in 49 wells. As some wells are deviated, a total of 54 temperature series are available. However, to obtain a reliable value, a correction is necessary. The correction method is performed on the deeper measurement, the Bottom Hole Temperature (BHT). The principle is to fit a regression curve to the time series BHT. We are using the Instant Cylinder Source (ICS) method from Goutorbe et al. (2007) allowing to obtain a close to equilibrium temperature.

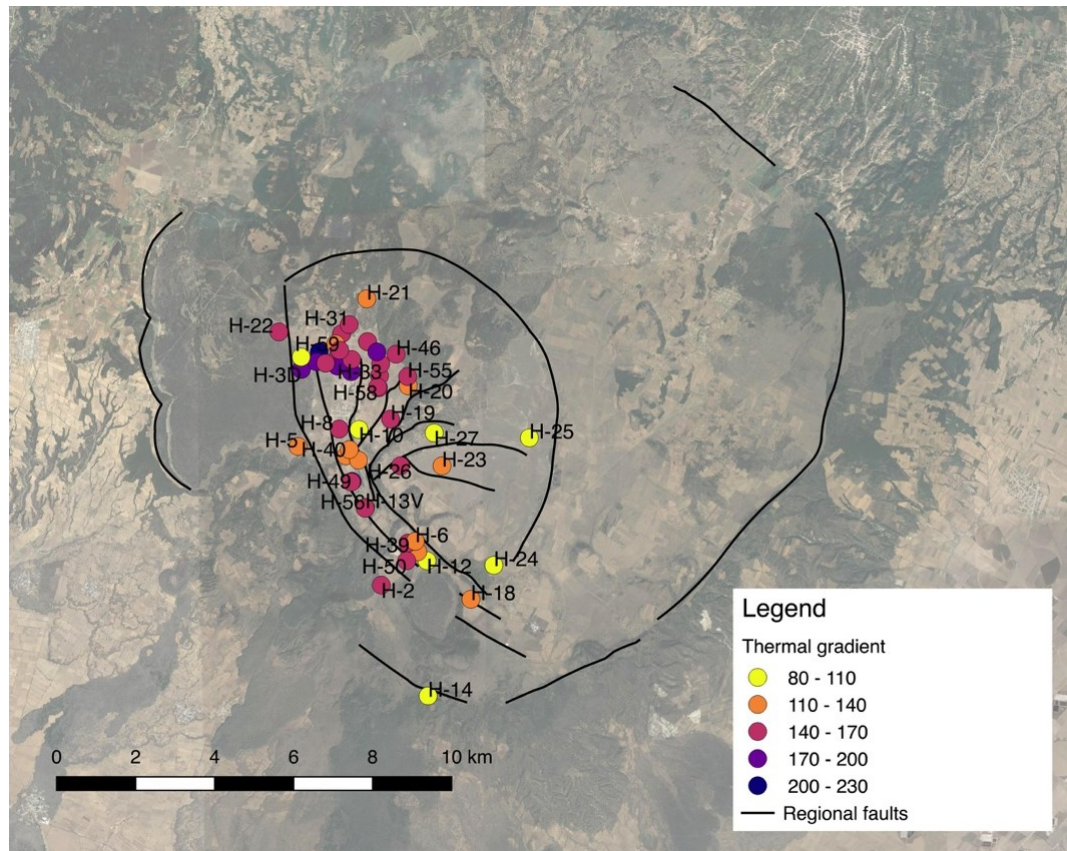


Figure 2: Thermal gradient from the equilibrium BHT temperature in the wells in Los Humeros.

The result obtained noticeably shows that the highest temperatures are in the northern part of the inner caldera and follow the main SW-NE faults. It is also obvious that the temperatures are widely irregular and are not in clusters (Fig. 2).

For the first step of the modelling only 3 wells have been used as they have been considered as been in purely convective mode and therefore where of importance to support the characterisation of the magmatic contribution to the thermal structure. For the later stages, 48 wells have been used, excluding 6 wells with an altitude that was consider has giving uncertain results.

2.1.2 Geological model

The geological model used is the regional model from Calcagno et al. (2018). The starting point to develop this model is the map published by Carrasco-Núñez et al. (2017), this map also defines the lateral extension of the model. In addition to the valuable initial information from the authors of Carrasco-Núñez et al. (2017), the work of Norini et al. (2015) has provided further constrains and knowledge. The contribution of the well information from CFE (Comisión Federal de Electricidad) has also been significant in defining the volcanoclastic sequence in depth. Figure 3 show the geological model used for the thermal modelling of Los Humeros.

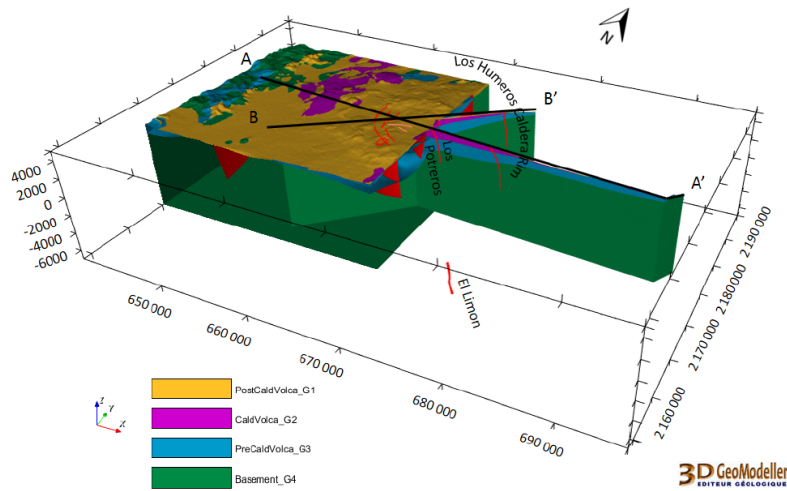


Figure 3: Geological model used for the thermal modelling of Los Humeros.

The model consists of 128 by 128 by 52 cells (851,968) and has a physical size of 56,000 m x 36,000 m x 20,000 m in x,y,z . The top of the model is located at 5,000 m above sea level (-5,000 m) and extends to 15,000 m below sea level (15,000 m). The model has a horizontal resolution of 437.5 m for x and 281.25 m for y . The vertical resolution of the model changes with depth: for a depth z of 1,000 meter below sea level, the cell size is 250 m and at deeper levels, it is 500 m. The model consists of five main layers based on the preliminary geological model of Evanno (2017) and Calcagno et al. (2018).

2.1.3 Geological model

Los Humeros Volcanic Complex (LHVC) is at the northern end of the Serdán-Oriental Basin (SOB), as such it is surrounded by height to the south-west (Cofre de Perote) and north-east (exhumed system between Acoculco and Los Humeros). The feed of the Los Humeros geothermal system is mostly carried by the Cretaceous and Jurassic limestone that are below the volcanic deposit sequences. The heights surrounding the LHVC, where the limestone outcrop such as in the exhumed system to the northwest or where is it shallow below highly permeable volcanoclastic sediment such as near Cofre de Perote to the south east. In addition, the Basin is tilted to the north-east, creating the main flow direction in the limestone.

According to the work of T. Kretzschmar (pers. communication), the total watershed (Fig. 4) extend that recharges the system covers an area of 10,227 km², which is more that the extend of the modelled area (2,035 km²), and is composed of 6 individual watersheds. The total volume of water collected in these watersheds is 10.2×10^9 m³ but the recharge of the Los Humeros geothermal system is only 2% (204.5×10^6 m³).

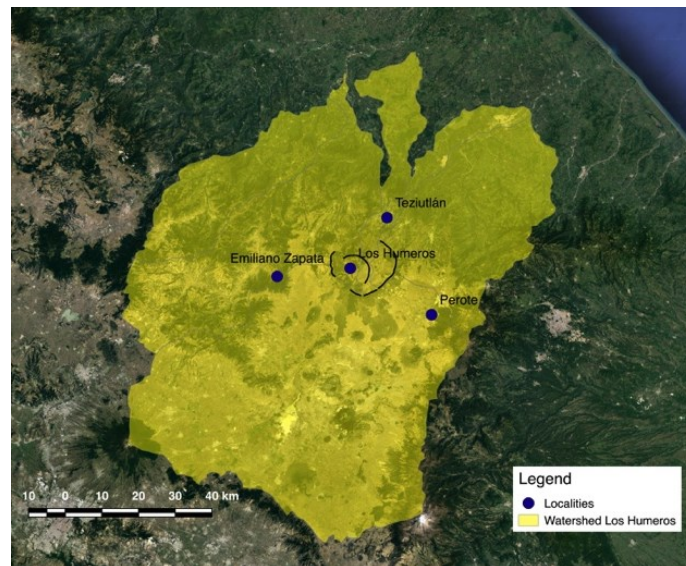


Figure 4: Los Humeros watershed.

The implication for the model is that all the recharge for the modelling is being made through the border via the limestone (blue polygon on Fig. 5). The reason for not having the recharge on the complete tour is due to the tilt of the limestone toward the northeast. However, the caldera is the outflow and the variability on the flow will be part of the adjustment made through the model iteration.

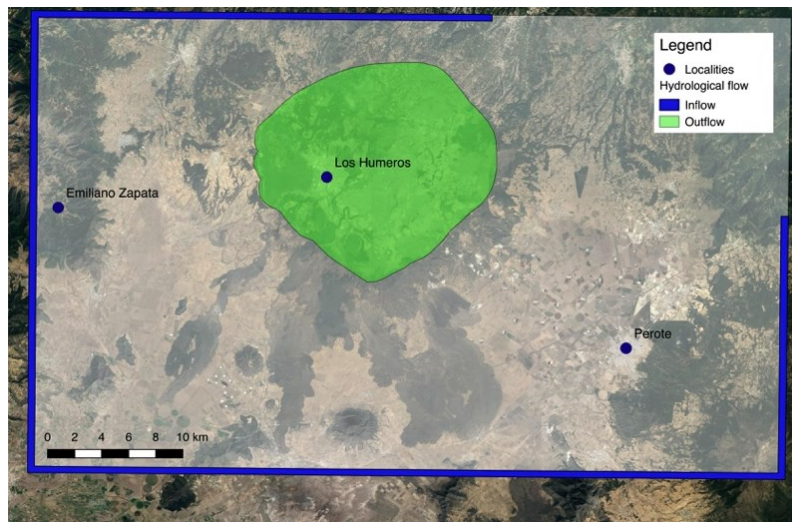


Figure 5: Inflow and Outflow for the Los Humeros.

2.2 Methodology

The backbone of the methods used for calculating the thermal state of the Los Humeros area are based on an extension of the work of Limberger et al. (2018). In this work, the thermal state of the lithosphere is estimated, assuming steady-state conditions and conductive heat transfer only. For the Los Humeros model, the thermal field was initially calculated with a multi-1D, steady-state conductive thermal model to initialize temperature- and pressure-dependent thermal properties, before calculating the 3D steady-state conductive forward thermal model. This 3D steady-state conductive forward model is used as a reference model and serves as a base for superposition of (a combination of) non-steady-state and/or advective effects.

For all the models, 25°C and 600°C were assumed for the upper and lower boundary conditions after Verma and Gómez-Arias (2013; 2014). To study the effect of non-steady-state and/or advective effects, we used inverse modelling on a selection of temperature measurements to find a suitable range for the magma chamber emplacement depth, regional groundwater fluxes, and local advection.

Each of the layers in the model consists of a single lithology or of a mixture of lithologies. Bulk thermal conductivity for each layer is iteratively calculated, taking into account compaction effects and temperature/pressure dependence. Bulk radiogenic heat production is a fixed number for the matrix of each lithology

2.2.1 Magmatism

The effect of magmatism is incorporated by emplacing a magma body at an emplacement time, which instantaneously modifies the temperature of the grid. Subsequently for the remainder of the time the transient heat equation is numerically solved deploying a Runge-Kutta method (Van Wees et al., 2009). The Latent heat of the magma chamber is incorporated. This can be done incorporating a temperature dependent heat capacity or by adopting a correction for the emplacement temperature of 200 °C in agreement with the latent heat energy released during cooling (Spear and Cheney, 1993; Paterson et al., 1998). Close to the magma chamber the latter results in an exaggeration of the predicted temperatures during cooling. However further away, in the depth range of temperature observations this has no effect. The geometry of the magma body is represented by an oblate spheroid, with the short axis vertical and the symmetry around the vertical axis. In the modelling a key uncertainty is the size as well as the depth of the magma chamber. These parameters strongly control the spatial extent and the geothermal gradient of the thermal anomaly observed in the Acoculco and Los Humeros geothermal reservoirs. Therefore, the thermal models presented below allow to constrain these parameters both for Acoculco and Los Humeros through finding best fit of model predictions to the temperature observations.

2.2.2 Hydrothermal fluxes

Superposed on the magmatic transient effects after its emplacement time, the hydrothermal fluid flow can strongly affect the thermal field. In the Los Humeros field, we have investigated the potential effect of the hydrothermal flow, by adopting a very simple hydrogeological model. Its prime aim has been to show the strong influence of deep-water circulation on the thermal field. The hydrothermal flow field is calculated in the 3D model with the following boundary conditions and flow properties:

- A deep (carbonate) flow zone is assumed (in blue, Fig. 6),
- The surface influx and outflux feeding to the deep flow zone is represented through a single input grid with $Q(x,y) > 0$ and $Q(x,y) < 0$ corresponding to the hydrological recharge (q_r) or discharge value (q_d) respectively. The sum of these fluxes is zero.
- The Q -values are chosen such that they represent flux values which are thought to be connected to the deep flow circulation in the carbonates. At x,y location where influx or outflux is present, the permeable layer is therefore overlain by a vertical flow conduit marked by a very high vertical and horizontal permeability (K_v/K_h) ratio.
- The flow field is solved using eq. 2.4 for steady state conditions using Q and the permeability field above, and assuming no flow in or out of the model, except for $Q(x,y)$ at surface.

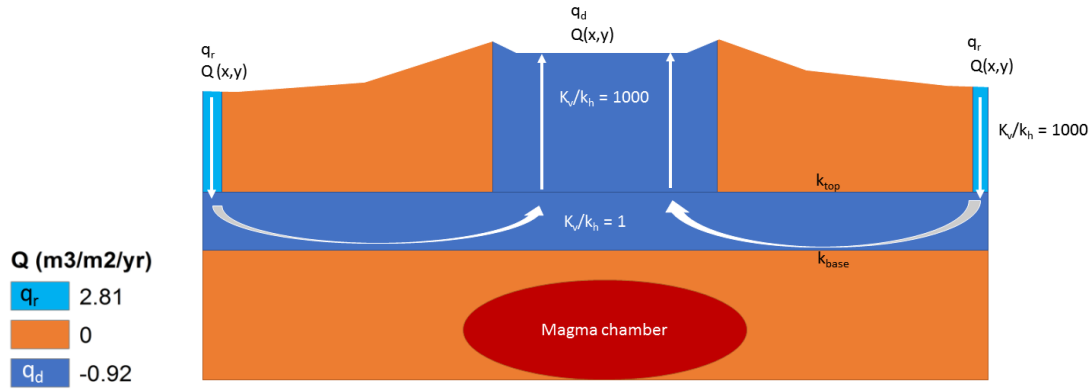


Figure 6: Schematic section of the recharge and discharge boundary conditions and the simplified hydrogeological model to calculate the 3D flow field

2.3 Model results

The Los Humeros geothermal field has been in operation for several decades. About 60 wells have yielded important information on reservoir properties and the thermal state of the region. This has allowed estimates on emplacement depth, temperature, and the size of the magmatic heat source. Our numerical approach solves the transient heat and mass transport equations to estimate the present-day temperature distribution around a single magmatic heat source, associated with the ~0.164 Kya ignimbrite eruption (Carrasco-Núñez et al. (2018)). Later magmatism, associated with post-caldera resurgence has not been taken into account.

The two models we present here combine magmatism and groundwater flow (Fig. 7). Model A combines the regional effect of deep-water circulation with spatial variation of flow (q_d and q_r) in the caldera zone, and the emplacement of a magmatic heat source at 5 km below sea level. The best fit was obtained by scaling the natural flux Q with 0.5, before shifting the local discharge q_d by a value randomly sampled from a uniform distribution between +5 and -5. The sum of the total q_d and q_r is kept at zero by adjusting the q_r accordingly. To incorporate the effect of locally adjusted surface sources (q_d and q_r) into each thermal model run, the hydrological model was updated and the resulting fluxes used as input for the thermal model. Model B differs from model A by a shallower magma emplacement of 2.5 km below sea level and scaling the natural flux Q with 0.1, before shifting the local discharge q_d by a value randomly sampled from a uniform distribution between +2.5 and -2.5.

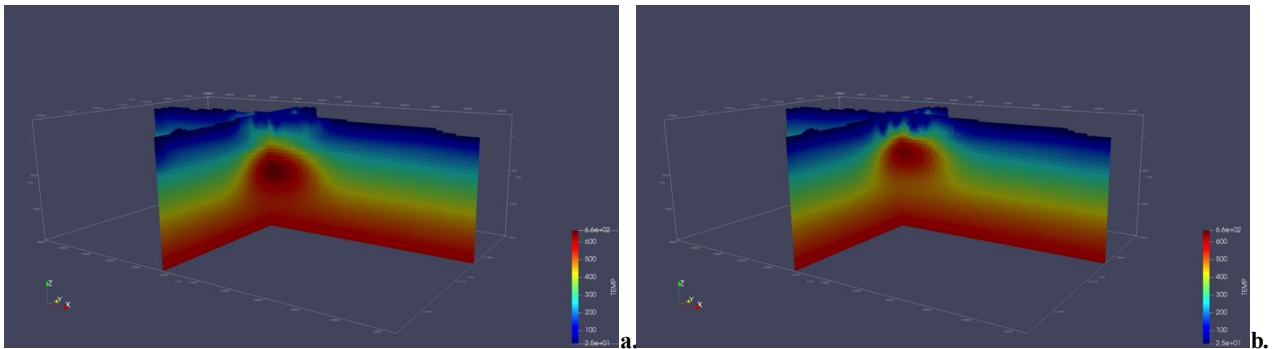


Figure 7: N-S and W-E cross sections through the thermal model based on the mean calculated temperatures after stochastically varying the hydro fluxes. (a) model, the emplacement depth of the heat source was set at 5 km below sea level, while the thickness of the hydraulically conductive layer was increased to 5 km. (b) model B, the emplacement depth of the heat source was set at 2.5 km below sea level, while the thickness of the hydraulically conductive layer was kept at 1 km.

Both models show a reasonable fit with the wells used for the inversion (Fig. 8). The main difference is that model A underestimates the temperature for most of the misfit well (outside the predefined $\pm 20^\circ\text{C}$ error bandwidth), while model B mostly overestimates temperatures for these misfit wells. What becomes clear from the misfit maps is that over- and underestimated values are in some cases very close-within one or two model cells-to each other. This could indicate that the model horizontal and vertical resolution might be a limiting factor for finding the best fit, as it limits the capability to simulate advective heat transfer via small-scale faults and fractures.

Other limiting factors are the single layer and vertical conduit, the input fluxes, the assumed ratio between precipitation and infiltration, and the onset of hydrothermal activity at 5 Kya. The evolution of the Los Humeros Volcanic Complex also consists of more phases than the single magmatic heat source emplacement assumed in these models (Giordano et al., Task 3.1; Carrasco-Núñez et al. (2018)). Multiple heat sources, rejuvenation of existing heat sources, and bimodal volcanism could have a significant impact on the results.

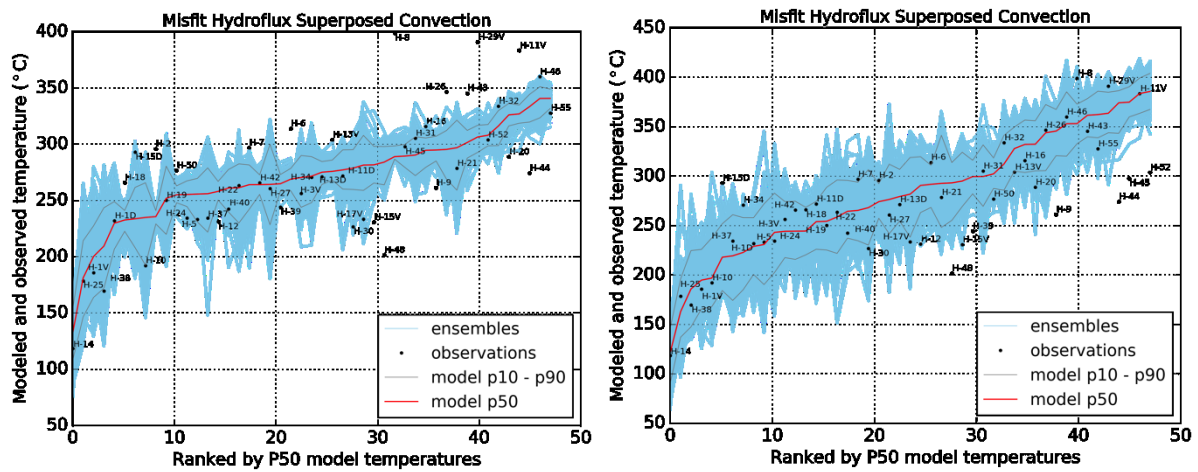


Figure 8: Rank plots of modeled temperature (lines) and observed temperatures (dots) at the well locations, ranked by the modeled P50 values of temperature at the well locations (middle). On the left, model A on the right, model B.

3. REGIONAL TEMPERATURE STRUCTURE OF ACOCULCO

3.1 Data

3.1.1 Temperature

The Comisión Federal de Electricidad (CFE) drilled two exploratory wells not too far from each other in the area of Acoculco caldera: the well EAC-1 in 1995 and the well EAC-2 in 2008 reaching a final depth of 1810 and 1,900 m, respectively. CFE acquired time-temperature series during the thermal recovery of the boreholes enabling the extrapolation of the static temperatures by the application of the well-known Horner Plot method. When 3 or more time-temperature couples of data are available at the same depth, a linear best fitting method including *a priori* standard errors in temperature ($\pm 1^\circ\text{C}$) and time (± 0.25 hrs) observations has been applied (York et al. 2004). This regression method allowed the estimation of the uncertainties on the extrapolated temperatures. The best straight-lines using the regression of York et al. (2004) gave similar results respect the standard linear regression being the differences as low as 1°C . The average uncertainty on the extrapolated temperatures is of the order of $\pm 9^\circ\text{C}$.

Generally, the thermal logs have a spatial resolution of 200 m down to 1,000 m and of 50 m from 1,000 m down to the bottom hole. At each measurement point, 4 temperatures have been recorded after shut-in times of 6 hrs, 12 hrs, 18 hrs and 24 hrs. In the EAC-1 well additional measurements taken after 288 and 312 hrs (12 and 13 days, respectively) were also recorded at fewer points. In the upper section of both the wells, approximately 1,000 m thick, the recorded time-temperature series suddenly decrease as function of increasing shut-in time. This time-dependent trend can be related with the thermal effect of the circulating drilling mud that cooled the bottom hole during drilling and then carried out the heat toward the well-head warming the upper section of the borehole. The magnitude of this thermal effect decreases with depth and nearby 800-1,000 m vanishes. Below 1000 m the time-temperature series shown a regular growth as function of shut-in time.

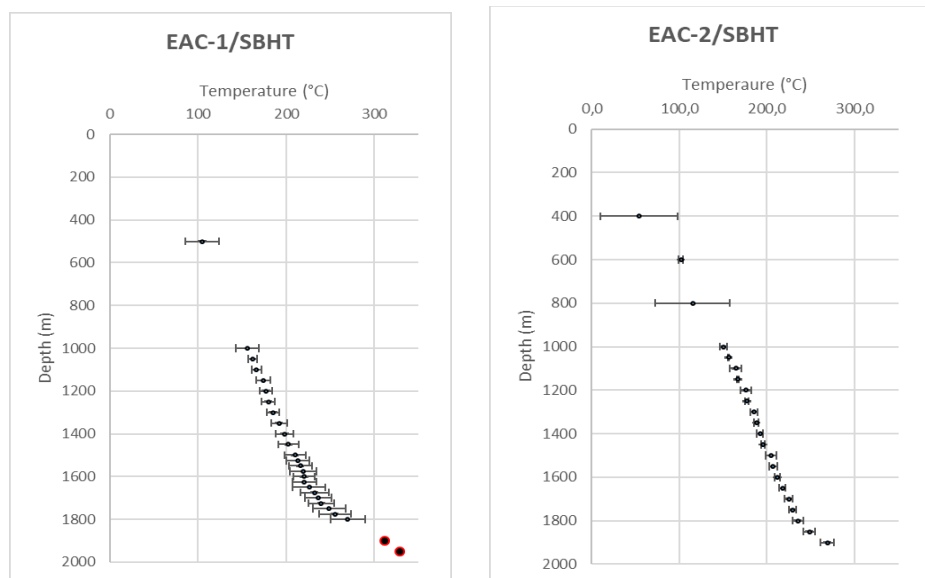


Figure 9: Static temperature profiles with error bars (black dots and bars) of EAC-1 (left) and EAC-2 (right) wells. In EAC-1 well the two deepest temperatures came from the application of the Horner method to 2 time-temperature couples measured after 288 and 312 hrs since the circulation of the drilling mud stops.

In both the wells, the resulting static profiles show common features (Fig. 9): i) a mainly conductive heat transport dominates in the underground and ii) the geothermal gradients show an increase nearby 1.75 – 1.80 km increasing from 106 – 117 °C/km in the upper section to 275 – 355 °C/km in the deeper one.

3.1.2 Geological model

The Acoculco area was modelled at a regional scale (Fig. 10). For a detailed description of the Acoculco geomodel, please refer to Calcagno et al. (2018).

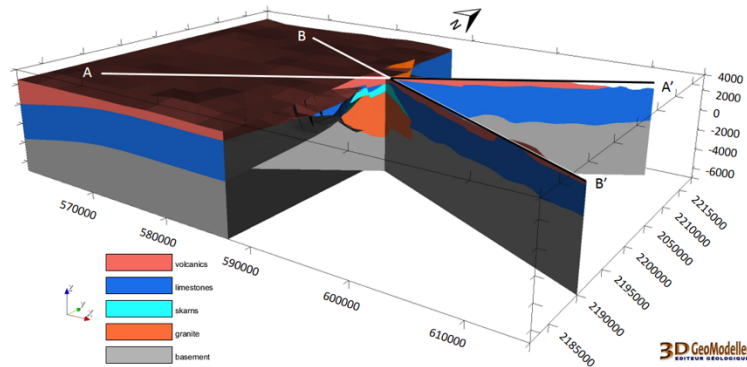


Figure 10: The Acoculco regional geomodel of the five geological groups listed at bottom. Coordinate system is WGS84/UTM zone 14N. Figure taken from Calcagno et al. (2018).

The geological map from Avellán et al. (2018) is the main references to set up the geomodel. In addition, the Comisión Federal de Electricidad (CFE) has provided a general geological description of two exploration wells. Moreover, other information on the two exploration wells and on the geological setting were retrieved from literature (e.g. López-Hernández et al., 2009; Lorenzo-Pulido et al. 2010). Fieldwork, mainly done by Liotta's team, was also used. A selection of the main faults to be modelled was done. They all have a maximum extension of four kilometres (below ground level) corresponding to the interpretation of the brittle-ductile transition. For the modelling process, the geological formations are described as five groups (see Fig. 10). The Digital Elevation Model (DEM) is provided by INEGI (Instituto Nacional de Estadística Geografía e Informática). The geomodel at regional scale (56 km x 37 km x 10.5 km, i.e. down to 7 km below sea level) presents five geological groups: basement, granite, skarns, limestones, and volcanics (Fig. 10). The geological map (Avellán et al., 2018) was re-interpreted accordingly. Two geological cross-sections were drawn to interpret the deep structures. They serve as reference for the geological interpretation. Nine complementary cross sections were drawn according to the two references cross-sections to ensure a coherent interpretation, for instance in terms of geological formations thickness.

3.2 Methodology

Once a geological model consistent with the available data is made, it can form the framework of the subsequent regional thermal model. Solving numerical simulations of heat and mass transfer in porous media is critical in order to assess the geothermal potential. With the aim to evaluate the regional thermal structure, the concept of lithothermal unit is adopted and the different geological formations were grouped on the basis of their thermal and hydraulic properties. The lithothermal units are treated as a homogeneous and downward anisotropic porous material (Pasquale et al. 2011) in which mixing laws were applied to estimate the effective thermal and hydraulic properties accounting for the in-situ conditions (depth and temperature). The definition of the Acoculco geothermal field considered five fundamental units, from the top to the bottom i) the cap-rock unit, ii) the limestone unit, including the skarn, iii) the basement unit, iv) the old intrusive body and v) the young intrusive body set inside the old one. The thermal properties of the main lithothermal units were assigned from literature data (Canet et al. 2015b) and according to new confidential data released in the framework of GEMex. The physical parameters and the constitutive laws used to describe the macroscopic behaviour of the water-rock system are reported.

The time-dependent heat and mass transfer equations were solved using the FEM method within a 3-D numerical domain that include a layered crust 10 km thick. As boundary conditions, we applied specific temperature-dependent thermal properties of the rocks, a constant surface temperature, a fixed heat flux at the base of the model and a time-dependent heat flux across the young intrusion boundaries. Not many heat flow data exist for the area of study, a value of 73 mW/m² is reported in the compilation by Pollak et al (1993). In addition, a new heat flow map of Mexico has been recently published by Prol-Ledesma et al. (2019). Accounting for the radiogenic heat contribution of the upper crustal rocks, a final value of 60 mW/m² was set at the base of the numerical domain.

The regional thermal model was set up with the aim to test the hypothesis about the existence of a recent and relatively shallow magmatic intrusion that induced in the overlaying formations a transient thermal signal. Large computational source allowed to solve the three components of the velocity field, the pressure and the temperature on a mesh grid counting more than $5 \cdot 10^6$ nodes. We approximated the complex dike and/or laccolite magmatic system with a simpler geometrical shape, i.e. a spheroid. The prolate or oblate spheroid mimics the dike or laccolite ensemble, respectively. Via a Monte Carlo approach, we investigated a number of possible scenarios by varying 1) the emplacement temperature (T_{mag}), 2) the aspect ratio (α), 3) the radius (R) as well as 4) the spheroid depth (Z).

3.3 Result of the thermal model

The Acoculco geothermal system lies within the Tulancingo–Acoculco Caldera Complex (Sosa-Ceballos et al., 2018; López-Hernández et al., 2009) sited in the eastern portion of the Trans-Mexican Volcanic Belt. This volcanic complex formed in the Pliocene time (3.0–2.7 Ma) with the formation of the Tulancingo Caldera. A second event in the Pleistocene time (1.7–0.24 Ma) drove the

development of the Acoculco Caldera within the older depression. According with the measured high $^3\text{He}/^4\text{He}$ values ($R/R_a = 6.3$, Polak et al., 1982), which suggest the presence of an active deep-seated magmatic source; we explained the actual trend of the measured temperature profiles as the shallow expression of a recent magmatic event.

The emplacement depth and temperature as well as the size of the magmatic body are unknown. Our numerical approach consisted in solving the transient heat and mass transport equations in order to forecast the present-day temperature distribution around a hypothetical, and recent magmatic intrusion. The choice of solving for a dominant conductive heat transfer mechanism by setting very low permeability values to the rocks ($K < 10^{-18} \text{ m}^2$) is supported by the thermal evidences recorded in the wells and the observed pervasive secondary mineralization both at surface and in the cores that reduced the permeability of the rocks.

We simulated the evolution of the thermal structure as consequence of a fast emplacement of magma at time t_1 having a fixed temperature T_{mag} which persist in the mid-to upper crust until time t_2 . The initial conditions correspond to the steady-state conductive temperature distribution evaluated for a basal heat flow of 60 mW/m^2 . The time-dependent solutions are computed every 1 kyr and the length of the simulation is 155 kyr. The magmatic body starts to warm the overlying rocks as soon as it emplaced at depth. The thermal wave moves upward controlled by the thermal diffusivity structure. The thermal load is provided by the heat source for a time interval of 100 kyr. At time t_2 the heat source starts to cool and the release of the latent heat of crystallization has been considered. The heat source has been parametrized through a Monte Carlo optimization procedure minimizing the misfit between the measured and simulated temperatures.

The normalized root-mean square error (NRMSE) has been computed globally, i.e. using as control points all the 46 borehole temperatures (24 from EAC-1 well and 22 from EAC-2 well). Low NRMSE values are observed in the cooling stage for time larger than 10 kyr. These are related to a better data fitting in the upper section of the thermal profiles but not in the lowermost section where a change in the thermal gradient is observed. The characteristic convex upward trend of the thermal profiles is simulated during the warming phase and as soon as the cooling phase starts. In Figure 18 the thermal profiles evaluated along the EAC-1 well at different times during the warming and cooling phases are shown. As regards the timing, if the heat source is still active and we fall into the warming stage, the thermal wave required about 50-80 kyr to reach the depth of the bottom holes. Instead, if we fall in the cooling stage, the intrusion was active up to about 5-6 kyr ago or less. Choosing the scenarios that give a $\text{NRMSE} < 4$, the emplacement temperature and the top of the intrusion are $850 \pm 50^\circ\text{C}$ and $2300 \pm 400 \text{ m}$ below ground level, respectively. Although a preferred narrow shape of the dikes system gives the better data fitting, we need supplementary boreholes in the area of study or other geophysical data in order to better constrain the lateral extent of the thermal anomaly.

We would stress that as the Acoculco geothermal field has not been yet explored in detail, large uncertainties may exist due to the lack of data. The actual regional model represents the best prediction using the available information from literature and from other GEMex Tasks.

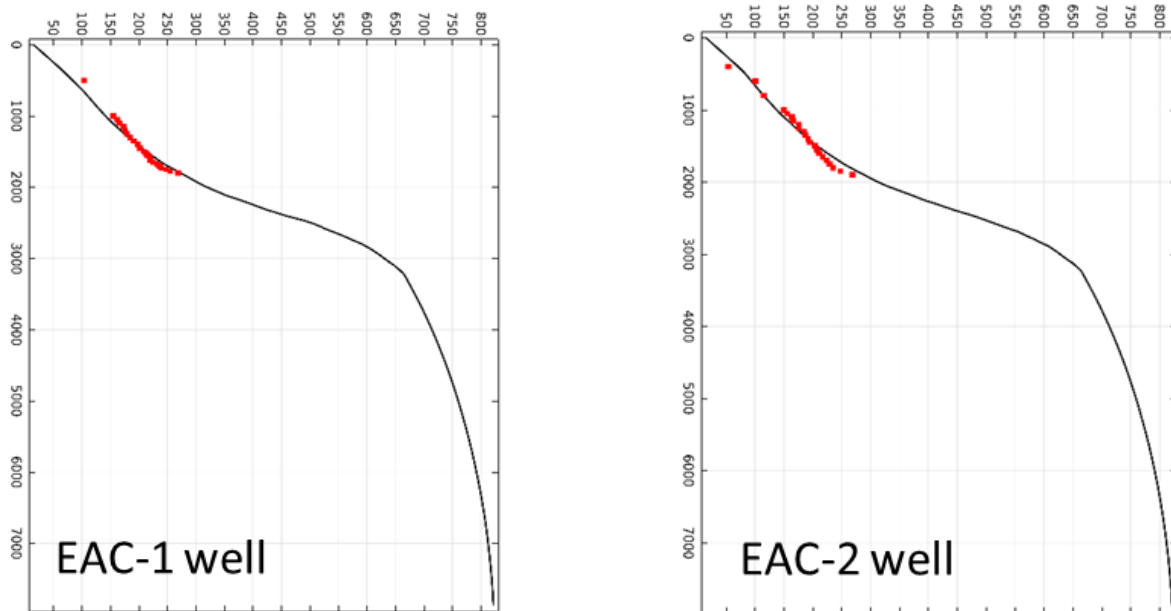


Figure 11: Thermal profiles evaluated as soon as the intrusion starts to cool for an initial emplacement temperature of 850°C and its top set at 2300 m b.g.l.

ACKNOWLEDGMENT

This paper presents results of the GEMex Project, funded by the European Union's Horizon 2020 research and innovation programme under grant agreement No. 727550, and by the Mexican Energy Sustainability Fund CONACYT SENER, Project 2015-04-268074. More information can be found on the GEMex Website: <http://www.gemex-h2020.eu>. A special thanks is due to CFE (Comisión Federal de Electricidad) for providing numerous information concerning their sites.

REFERENCES

- Avellán, D. R., Macías, J. L., Layer, P. W., Cisneros, G., Sánchez-Núñez, J. M., Gómez-Vasconcelos, Pola, A., Sosa-Ceballos, G., García-Tenorio, F., Reyes-Agustín, G., Osorio-Ocampo, S., García-Sánchez, L., Mendiola, F., Martí, J., López-Loera, H., and Benowitz, J., 2018. Geology of the Late Pliocene – Pleistocene Acoculco caldera complex, eastern Trans-Mexican Volcanic Belt (México), J. Maps.
- Calcagno, P., Evanno, G., Trumpy, E., Gutiérrez-Negrín, L. C., Macías, J. L., Carrasco-Núñez, G., and Liotta, D., 2018. Preliminary 3-D geological models of Los Humeros and Acoculco geothermal fields (Mexico) – H2020 GEMex Project, Adv. Geosci., 45, 321-333.
- Canet, C., Hernández-Cruz, B., Jiménez-Franco, A., Pi, T., Peláez, B., Villanueva-Estrada, R. E., Alfonso, P., González-Partida, E., and Salinas, S., 2015a. Combining ammonium mapping and short-wave infrared (SWIR) reflectance spectroscopy to constrain a model of hydrothermal alteration for the Acoculco geothermal zone, Eastern Mexico, Geothermics, 53, 154–165.
- Canet, C., Trillaud, F., Prol-Ledesma, R. M., Gonzalez-Hernandez, G., Pelaez, B., Hernandez-Cruz, B., and Sanchez-Cordova, M., 2015b. Thermal history of the Acoculco geothermal system, eastern Mexico: Insights from numerical modeling and radiocarbon dating. Journal of Volcanology and Geothermal Research, 305, 56–62.
- Carrasco-Núñez, G., Bernal, J., Dávila, P., Jicha, B., Giordano, G., and Hernández, J., 2018. Reappraisal of Los Humeros Volcanic Complex by New U/Th Zircon and 40Ar/39Ar Dating: Implications for Greater Geothermal Potential. Geochem. Geoph. Geosy., 19, 132–149.
- Carrasco-Núñez, G., López-Martínez, N., Hernández, J., and Vargas, V., 2017. Subsurface stratigraphy and its correlation with the surficial geology at Los Humeros geothermal field, eastern Trans-Mexican Volcanic Belt. Geothermics, 67, 1–17.
- Evanno G., 2017. Final Dissertation of Master Degree, 3D Preliminary Geological Modelling of the Los Humeros Geothermal Area (Mexico), ENAG/MFE-088-GB-2017.
- Giordano, G., Lucci, F., Rosetti, F., Urbani, S. (in prep.): GEMex Task 3.1 Update on the volcanological conceptual model of Los Humeros geothermal field.
- Goutorbe, B., Lucazeau, F. & Bonneville A., 2007. Comparison of several BHT correction methods: a case study on an Australian data set. Geophysical Journal International, 170, 913-922.
- Limberger, J., van Wees J. D., Tesauro M., Smit J., Bonté D., Békési E., Pluymaekers M., Struijk M., Vrijlandt M., Beekman F., and Cloetingh S., 2018. Refining the thermal structure of the European lithosphere by inversion of subsurface temperature data, Global and Planetary Change, 171, 18-47.
- López-Hernández, A., García-Estrada, G., Aguirre-Díaz, G., González-Partida, E., Palma-Guzmán, H., and Quijano-León, J. L., 2009. Hydrothermal activity in the Tulancingo–Acoculco Caldera Complex, central Mexico: Exploratory studies, Geothermics, 38, 25 279–293.
- Lorenzo-Pulido, C., Armenta-Flores, M., and Ramírez-Silva, G., 2010. Characterization of the Acoculco Geothermal Zone as a HDR System, GRC Transactions, 34, 369–372.
- Norini, G., Groppelli, G., Sulpizio, R., Carrasco-Núñez, G., Davila-Harris, P., Pelliccioli, C., Zucca, F., De Franco, R., 2015. Structural analysis and thermal remote sensing of the Los Humeros Volcanic Complex: implications for volcano structure and geothermal exploration. J. Volcanol. Geotherm. Res. 301, 221–237.
- Pasquale, V., Gola, G., Chiozzi, P. and Verdoya, M., 2011. Thermophysical properties of the Po Basin rocks. Geophysical Journal International, 186, 69-81.
- Paterson, S., Fowler jr, T., Schmidt, K., Yoshinobu, A., Yuan, E., and Miller, R., 1998. Interpreting magmatic fabric patterns in plutons. Lithos, 44, 53–82.
- Polak B.G., Prasalov., E.M, Kononov, V.I., Verkovsky, A.B, González, A., Templos, L.A., Espíndola, J.M., Arellano, J.M, and Manón, A., 1982. Isotopic composition and concentration of inert gases in Mexican hydrothermal systems. Geofísica Internacional, 21, 193–227.
- Pollack, H. N., Hurter, S. J., and Johnson, J. R., 1993. Heat - flow from the Earth’s interior—Analysis of the global data set, Rev. Geophys., 31, 267–280.
- Prol-Ledesma, R. M. and Morán-Zenteno, D. J., 2019. Heat flow and geothermal provinces in Mexico. Geothermics, 78, 183-200.
- Sosa-Ceballos, G., Macías, J. L., Avellán, D. R., Salazar-Hermenegildo, N., and Boijseauneau-López, M. E., 2018. The Acoculco Caldera complex magmas: Genesis, evolution and relation with the Acoculco geothermal system. Journal of Volcanology and Geothermal Research, 358, 288–306.
- Spear, F., and Cheney, J., 1993. Metamorphic Phase Equilibria and Pressure-Temperature-Time Paths. Mineralogical Society of America, Washington, ISBN 0-939950-34-0.
- Van Wees, J. D., Bergen, F. V., David, P., Nepveu, M., Beekman, F., Cloetingh, S. and Bonté, D., 2009. Probabilistic tectonic heat flow modeling for basin maturation: Assessment method and applications. Marine and Petroleum Geology, 26, 536–551.
- Verma, S. and Gómez-Arias, E., 2013. Three-dimensional temperature field simulation of magma chamber in the Los Humeros geothermal field, Puebla, Mexico. Appl. Therm. Eng., 52, 512–515.
- Verma, S., and Gómez-Arias, E., 2014. Optimal discretization time and mesh size in three-dimensional temperature field simulation in two Mexican geothermal fields, Puebla, Mexico. Geothermics, 51, 91–102.

York, D., Evensen, N. M., Martinez, M. L., and Delgado, J. D. B., 2004. Unified equations for the slope, intercept, and standard errors of the best straight line. *Am. J. Phys.*, 72, 367–375.